Dalton Transactions

ROYAL SOCIETY OF CHEMISTRY

PAPER

View Article Online
View Journal | View Issue

Cite this: *Dalton Trans.*, 2020, **49**, 5250

$[Re(\eta^6\text{-arene})_2]^+$ as a highly stable ferrocene-like scaffold for ligands and complexes†

Daniel Hernández-Valdés,[a] Frédéric Avignon,[a,b] Peter Müller,[a] Giuseppe Meola,[a] Benjamin Probst,[a] Thomas Fox,[a] Bernhard Spingler[a] and Roger Alberto *[a]

Received 27th February 2020,
Accepted 27th March 2020

DOI: 10.1039/d0dt00731e

rsc.li/dalton

Ferrocenes are versatile ligand scaffolds, complexes of which have found numerous applications in catalysis. Structurally similar but of higher redox stabilites are sandwich complexes of the $[Re(\eta^6\text{-arene})_2]^+$ type. We report herein routes for conjugating potential ligands to a single or to both arenes in this scaffold. Since the arene rings can freely rotate, the $[Re(\eta^6\text{-arene})_2]^+$ has a high degree of structural flexibility. Polypyridyl ligands were successfully introduced. The coordination of Co(II) to such a model tetrapyridyl-Re(I)-bis-benzene complex produced a bimetallic Re(I)–Co(II) complex. To show the stability of the resulting architecture, a selected complex was subjected to photocatalytic reactions. It showed good activity in proton reduction over a long time and did not decompose, corroborating its extraordinary stability even under light irradiation. Its activity compares well with the parent catalyst in turn over numbers and frequencies. The supply of electrons limits catalytic turnover frequency at concentrations below ~10 μM. We also show that other ligands can be introduced along these strategies. The great diversity offered by $[Re(\eta^6\text{-arene})_2]^+$ sandwich complexes from a synthetic point allows this concept to be extended to other catalytic processes, comparable to ferrocenes.

Introduction

Over the past decades, organometallic chemistry has found its way into many fields of science. Among the plethora of organometallic compounds, sandwich complexes have been studied in great depth in particular. Metallocenes are a focus (ferrocene), but arene sandwiches are less common and as such less studied. The first bis-arene sandwich, $[Cr(\eta^6\text{-}C_6H_6)_2]$, was reported by Fischer and Hafner *et al.* in 1955 by reducing $CrCl_3$ with $Al/AlCl_3$ in benzene.[1] Syntheses of bis-arene sandwich complexes are less straight than the ones of their cyclopentadienyl counterparts and the arene ligands are less stably bound to the metal centres due to their uncharged nature. Moreover, in many cases arene sandwich complexes are prone to oxidation and/or ligand loss.[2] Little attention was payed to $[Re(\eta^6\text{-}C_6R_6)_2]^+$ type complexes in particular. Although known since the Fifties,[3] little respective chemistry was developed over the past fifty years. Progress was recently made by Kudinov *et al.* and in our group by developing a high-yield, one step procedures from $[ReO_4]^-$ and $Zn/AlCl_3$ as activation/reduction agents.[4–6] Direct syntheses with functionalized arenes were reported as well, however, the high reactivity of $AlCl_3$ limits the compatibility to some aniline-type arenes.[7] Therefore, post-synthetic modifications are often required to introduce functionalities into the basic $[Re(\eta^6\text{-}C_6H_6)_2]^+$ framework, a comparable procedure as done with ferrocene. Because of its stability and great versatility in terms of derivatization, ferrocene has become landmark in organometallic chemistry and has played a fundamental role in many areas of chemistry. Numerous examples of applications in asymmetric catalysis, sensors, electroactive materials and anti-cancer agents abound in literature.[8–15] Developing similar concepts based on the $[Re(\eta^6\text{-}C_6H_6)_2]^+$ scaffold opens up a whole range of opportunities that we can explore.

In contrast to its neighbouring elements, we found that $[Re(\eta^6\text{-}C_6H_6)_2]^+$ type complexes are remarkably stable.[4,5,16] For instance, $[Re(\eta^6\text{-}C_6H_6)_2]^+$ does not decompose or lose benzene rings even when heated to 160 °C or when irradiated with UV light. $[Re(\eta^6\text{-}C_6R_6)_2]^+$ offers structural flexibilities in three dimensions as depicted in Scheme 1. Rotation around the rhenium axis, as well as tilting of pendent functionalities is possible without a notable energy barrier. The symmetry of all signals observed in the NMR spectra (see ESI†) supports the notion of free rotation at room temperature.[5–7,16,17]

Electrochemistry showed that Re(I) is reversibly oxidized at $E^\circ_{1/2} > +1.3$ V (Re^I/Re^{II}). Irreversible reductions take place at

[a]*Department of Chemistry, University of Zurich, Winterthurerstr. 190, CH-8057 Zurich, Switzerland. E-mail: ariel@chem.uzh.ch*
[b]*Département de Chimie, École Normale Supérieure, PSL Research University, 75005 Paris, France*

† Electronic supplementary information (ESI) available. CCDC 1957333–1957341. For ESI and crystallographic data in CIF or other electronic format see DOI: 10.1039/d0dt00731e

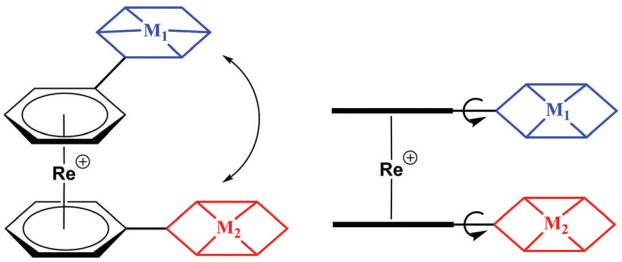

Scheme 1 Different degrees of freedom for the basic arrangement of $[Re(\eta^6\text{-}C_6H_6)_2]^+$ type complexes with two pendent coordinating modalities.

low potentials <−2.0 V, both *vs.* Ag/AgCl.[5,7] Compared to ferrocene, Re(I) bis-arene derivatives are much more difficult to oxidize and are generally stable against atmospheric oxygen (Fig. S1 and S2†).[18–20] These properties make $[Re(\eta^6\text{-}C_6H_6)_2]^+$ inert in several chemically interesting redox processes. A representative example is the reduction of H^+ to H_2 or CO_2 to CO, both of which require substantial, negative potentials.[21–26] Protons and/or CO_2 can be reduced by molecular catalysts in systems that commonly involve multiple components; photosensitizers, electron donors and proton shuttles. The $[Re(\eta^6\text{-}C_6H_6)_2]^+$ building block is an elegant way to combine two or more subunits in one molecule. Those subunits would be separated by a ring-ring distance of about 3 Å (Scheme 1), making communication between these two entities conjugated to the arene rings possible. This report shows that $[Re(\eta^6\text{-}C_6H_6)_2]^+$ is suitable for conjugating different ligands to the arenes by common synthetic arene modification strategies. To show retention of catalytic activity and non-interference of the $[Re(\eta^6\text{-}C_6H_6)_2]^+$ scaffold, the photocatalytic activity of a Re(I)–Co(II) heterobimetallic complex towards proton reduction is shown in detail and compared to the catalyst in its native form.

Results and discussion

Precursor syntheses

$[Re(\eta^6\text{-}C_6H_6)_2](OTf)$ (**1**) was mono or bis-lithiated with $LiN(i\text{-}Pr)_2$ (LDA) to form $[Re(\eta^6\text{-}C_6H_5Li)_2]^+$. Reactions with electrophiles lead to *e.g.* the respective bromides and carboxylates.[5] We extended the electrophiles to C_2Cl_6 or dimethylformamide (DMF) and prepared the mono-derivatized complexes $[Re(\eta^6\text{-}C_6H_6)(\eta^6\text{-}C_6H_5Cl)](PF_6)$ (**2a**$^+$) and $[Re(\eta^6\text{-}C_6H_6)(\eta^6\text{-}C_6H_5COH)](TFA)$ (**3a**$^+$) or their bis-functionalized analogues $[Re(\eta^6\text{-}C_6H_5Cl)_2](PF_6)$ (**2b**$^+$) and $[Re(\eta^6\text{-}C_6H_5COH)_2](PF_6)$ (**3b**$^+$) (Scheme 2, "a" always denominates mono-functionalization). The ratio of mono- and bis-functionalization can be controlled by varying the amounts of LDA, but the selective formation of only one product could not be achieved. The reaction with DMF produces a mixture **3a**$^+$ and **3b**$^+$ as main products but also alcohols and carboxylic acids groups on the arene rings due to the high reactivity of

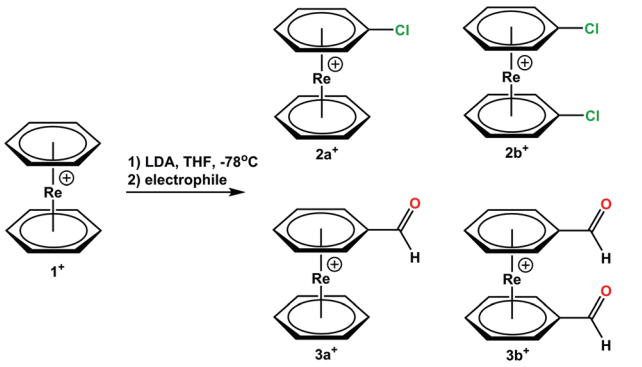

Scheme 2 Reaction scheme for the functionalization of $[Re(\eta^6\text{-}C_6H_6)_2]$ (OTf). Reaction conditions: (1) Lithiation/deprotonation 1.5–2.5 eq. of LDA, 1.5 h, −78 °C, THF; (2) *in situ* electrophilic attack 5 h, −78 °C, THF; electrophiles: C_2Cl_6 and DMF. Combined yields: (63.1% for **2a**$^+$, **2b**$^+$ and **2c**$^+$; 43.2% for **3a**$^+$ and **3b**$^+$).

these aldehydes. Since the solubilities of all products are very similar, clean separation of mono- and bis-aldehyde is challenging (full synthetic procedures and characterizations are given in the ESI†).

Preparative HPLC with an isocratic gradient: 5 : 95 $CH_3CN : H_2O$/TFA (0.1%) in 45 min, 40 mL min^{-1} leads to clean separation but UPLC-MS analysis evidenced that each fraction contained, besides **3a**$^+$ and **3b**$^+$, also the corresponding hydrate, supporting the high reactivity of the aldehyde groups attached to the electron poor arene rings. Obviously, there is an equilibrium established between these two species, which is more favourable for the aldehyde form.

Cyclovoltammetry (CV) of **3a**$^+$ and **3b**$^+$ was performed to study electrochemical properties (Fig. 1). Cyclovoltammograms for complexes **3a**$^+$ and **3b**$^+$ show irreversible oxidations at

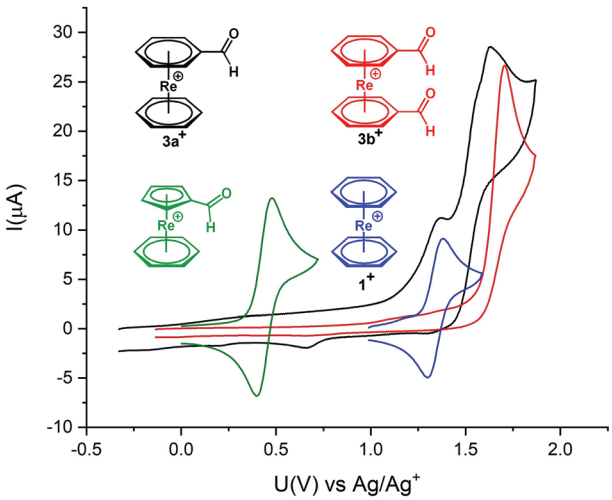

Fig. 1 Cyclovoltammogram of complexes **1**$^+$ (blue), **3a**$^+$ (black), **3b**$^+$ (red) and mixed sandwich arene-Cp aldehyde (green); acetonitrile, 0.1 M [TBA][PF_6] (electrolyte), glassy carbon working electrode (i.d. = 3 mm), Pt auxiliary electrode, and Ag/AgCl reference electrode, analyte concentrations 1 mM, voltage step: 6 mV, sweep rate: 0.1 V s^{-1}.

+1.63 V and +1.7 V (*vs.* Ag/AgCl), respectively. These oxidations are anodically shifted between +0.3 and +0.4 V relative to $\mathbf{1}^+$. The irreversible nature of the two oxidation processes in $\mathbf{3a}^+$ suggests a ligand- and a metal-based oxidation, as observed for other sandwich complexes with functionalities bound to the arene rings.[5,7] In $\mathbf{3b}^+$ with two electron-withdrawing groups on the arenes, the metal-based oxidation is probably beyond the solvent window and only the oxidation of the aldehydes occurs.

Meola *et al.* reported the mixed-ring complex $[Re(\eta^6\text{-}C_6H_6)(\eta^5\text{-}C_5H_4COH)]$ which also comprises an aldehyde.[17] It is interesting to compare the electrochemistry between this mixed-ring sandwich complex and $\mathbf{3a}^+$, both containing an aldehyde function. For $[Re(\eta^6\text{-}C_6H_6)(\eta^5\text{-}C_5H_4COH)]$, the reversible and thus metal-centred Re^I/Re^{II} oxidation takes place at +0.44 V (*vs.* Ag/AgCl) (Fig. 1). For $\mathbf{3a}^+$ the oxidation is irreversible and the first oxidation is ligand- and not metal-centred and shifted by about 1 V.

Conjugation of ligands to complexes $\mathbf{2a}^+$–$\mathbf{3b}^+$

The chloride and the aldehyde bearing arenes $\mathbf{2a}^+$–$\mathbf{3b}^+$ are highly susceptible for nucleophilic attack due to the electron-withdrawing effect of the cationic rhenium centre. To exemplify the conjugation of additional ligands to the $[Re(\eta^6\text{-arene})_2]^+$ frameworks, appropriate aromatic heterocycles such as pyrrole or pyrazole were chosen for forming C_{arene}–N_{ligand} bonds to complex $\mathbf{1}^+$. Pyrrole was deprotonated with NaH in dry THF.

Nucleophilic substitution of Cl^- in $\mathbf{2a}^+$ gave $[Re(\eta^6\text{-}C_6H_6)(\eta^6\text{-}C_6H_5\text{-pyrrol})](PF_6)$ ($\mathbf{4a}^+$) (Scheme 3) as the main product. The same procedure was applied to pyrazole, obtaining complex $\mathbf{5a}^+$ $[Re(\eta^6\text{-}C_6H_6)(\eta^6\text{-}C_6H_5\text{-pyz})](PF_6)$ in a 98% yield.

Complex $\mathbf{5a}^+$ carries a single sp^2-N as a potential coordination site. To extend the synthetic strategy towards bi- and multidentate ligands, the reaction of $\mathbf{2b}^+$ with 2-(1*H*-pyrazol-3-yl)pyridine (Hpyz-py) gave complex $[Re(\eta^6\text{-}C_6H_5\text{-pyzpy})_2](PF_6)$ ($\mathbf{6b}^+$) in almost quantitative yield. Complex $\mathbf{6b}^+$ has four nitrogen atoms for coordination to further metals centres. The crystal structure of $\mathbf{6b}^+$ shows that the pyzpy units are coplanar (Fig. 2).

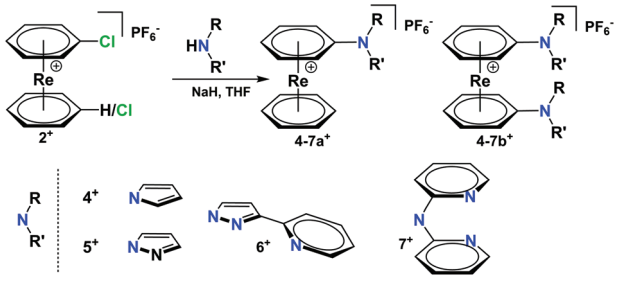

Scheme 3 Reaction scheme for conjugation of five and six-membered N-heterocyclic rings to $[Re(\eta^6\text{-}C_6H_6)(\eta^6\text{-}C_6H_5Cl)](PF_6)$ and $[Re(\eta^6\text{-}C_6H_5Cl)_2](PF_6)$. Reaction conditions: (1) Deprotonation of the N-heterocyclic rings or 2,2′-dipyridylamine with NaH, 2 h, 60 °C, THF; (2) nucleophilic substitution 3 h, 60 °C, THF.

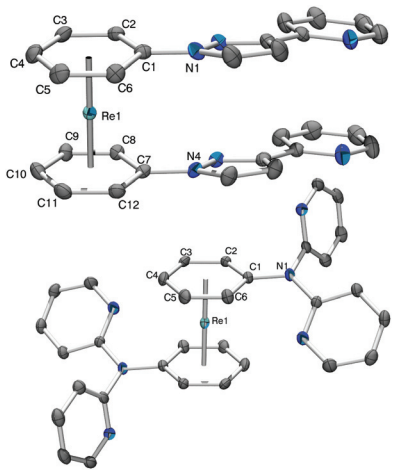

Fig. 2 ORTEP representation of cations $\mathbf{6b}^+$ (top) and $\mathbf{7b}^+$ (bottom). Hydrogen atoms and anions have been omitted for clarity; thermal ellipsoids represent 50% probability. Selected bond lengths (Å) for $\mathbf{6b}^+$: Re1–C1 2.276(2), Re1–C2 2.263(2), Re1–C3 2.246(2), Re1–C4 2.238(2), Re1–C5 2.231(2), R1–C6 2.237(2), Re1–C7 2.265(2), Re1–C8 2.260(2), Re1–C9 2.254(2), Re1–C10 2.237(2), Re1–C11 2.229(3), Re1–C12 2.240(2), C1–N1 1.400(3), C7–N4 1.405(3). For $\mathbf{7b}^+$: Re1–C1 2.310(3), Re1–C2 2.237(3), Re1–C3 2.231(3), Re1–C4 2.241(3), Re1–C5 2.252(3), R1–C6 2.275(3), C1–N1 1.409(3).

As obvious from the symmetry of the NMR signals, both rings in complex $\mathbf{6b}^+$ rotate in solution, therefore, the attached ligands can coordinate either individually to two metal centres or *via* both pyzpy units to a single metal centre. The symmetry of all NMR spectra and therefore the free rotation around the rhenium axis is found for all $[Re(arene)_2]^+$ synthesized by our group so far.[5–7,16,17,27]

Pyridines are prototypical ligands in many catalytic processes, *e.g.* for proton reduction in photocatalysis.[21,25] To extend the concept towards such polypyridyl ligands bound to the $[Re(\eta^6\text{-}C_6H_6)_2]^+$ scaffold, 2,2′-dipyridylamine (Hdipyam) was deprotonated with NaH in dry THF and reacted with $\mathbf{2a}^+$ and $\mathbf{2b}^+$ respectively. The two complexes $[Re(\eta^6\text{-}C_6H_6)(\eta^6\text{-}C_6H_5\text{-dipyam})](PF_6)$ ($\mathbf{7a}^+$) and $[Re(\eta^6\text{-}C_6H_5\text{-dipyam})_2](PF_6)$ ($\mathbf{7b}^+$) were obtained as PF_6^- salt in 74% and 23.7% yield, respectively after separation by preparative HPLC and precipitation with NH_4PF_6. Single X-ray crystal structures of both complexes confirm their authenticities (see Fig. 2 and ESI†).

Compounds $\mathbf{7a}^+$ and $\mathbf{7b}^+$ are stable but light sensitive and decompose in acetonitrile solution by ligand loss. After exposing acetonitrile solutions of complexes $\mathbf{7a}^+$ and $\mathbf{7b}^+$ to light, UPLC-MS evidenced a new peak with a *m*/*z* of 248.11, corresponding to the protonated form of phenyl-di-pyridylamine (see ESI†).

A chemically different synthetic route to form ligands directly on the arene rings in $[Re(\eta^6\text{-}C_6H_6)_2]^+$ starts from $\mathbf{3a}^+$. Aldehydes are convenient functionalities for a number of reactions, yielding *e.g.* terpyridine in a Kröhnke reaction in methanol at r.t.[28] Applying these conditions to the organometallic aldehyde $\mathbf{3a}^+$, the complex $[Re(\eta^6\text{-}C_6H_5\text{-terpy})(\eta^6\text{-}C_6H_6)](PF_6)$ ($\mathbf{8a}^+$) formed directly in the presence of acetylpyridine

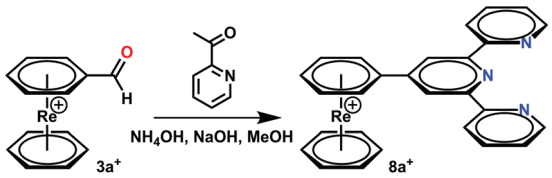

Scheme 4 Reaction scheme for conjugation of terpyridine to $[Re(\eta^6\text{-}C_6H_5COH)(\eta^6\text{-}C_6H_6)](TFA)$. Reaction conditions: Condensation reaction NaOH, 30 eq. acetylpyridine, 3 h, r.t., NH_4OH solution (25% in mass).

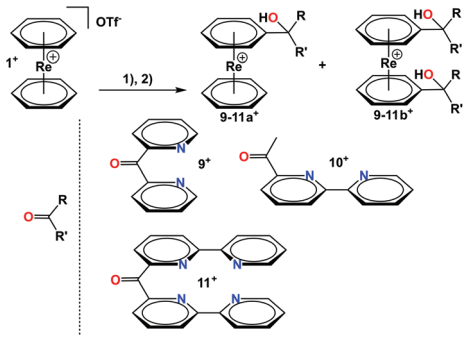

Scheme 5 Reaction scheme for conjugation of polypyridyl ligands to $[Re(\eta^6\text{-}C_6H_6)_2](OTf)$. Reaction conditions: (1) Lithiation/deprotonation 3.0 eq. of LDA, 1.5 h, −78 °C, THF; (2) addition to carbonyl 5 h, −78 °C, THF.

(Scheme 4). Precipitation with NH_4PF_6 gave complex **8a**$^+$ in good yields.

Ligand systems can also be directly conjugated to **1**$^+$ after lithiation as described before. For instance, mono- and bis-lithiated **1**$^+$ undergoes nucleophilic additions to carbonyl groups (Scheme 5). Several different keto-pyridines were employed in this way as electrophiles and products containing pendent ligands on one or both rings were isolated. Along this route, the mono and bis-substituted compounds **9a**$^+$/**b**$^+$, **10a**$^+$/**b**$^+$ and **11a**$^+$/**b**$^+$ could be obtained and were fully characterized (see ESI†).

In comparison with complexes **7a**$^+$ and **7b**$^+$, these new bis-arene based "ligands" are remarkably more stable; no decomposition was observed in the presence of light or coordinating solvents and they are all slightly water-soluble.

Synthesis of a bimetallic Re–Co catalyst

Compounds **11a**$^+$ and **11b**$^+$ are of special interest since Co(II) complexes of these tetra-pyridyl units represent a highly active class of catalysts for photocatalytic proton reduction.[29–33] To support the hypothesis that the $[Re(\eta^6\text{-}C_6H_6)_2]^+$ is a suitable scaffold, a Co(II) complex with **11a**$^+$ was prepared by reaction of 20 eq. $CoBr_2$ in MeOH with the metal-free precursor. Complete complexation was attained after a few minutes according to UPLC-MS (see Fig. S5 and S6†). Washing the product multiple times with Et_2O gave the pure product [**12a**]Br (Scheme 6).

The ^{1}H NMR spectrum in deuterated methanol showed broad signals between −10 ppm and +80 ppm, in agreement

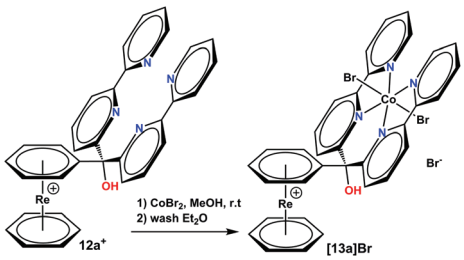

Scheme 6 Synthesis of complex [**12a**]Br. Reaction conditions: (1) 20 eq. $CoBr_2$, 1 h, r. t., in MeOH, (2) several washes with Et_2O.

with a paramagnetic nature of the complex. A single crystal X-ray structure analysis of **12a**$^+$ as trifluoromethanesulfonate (OTf) salt confirmed the formation of the Co(II) complex [**12a**]OTf (Fig. 3, full characterization in the ESI†).

The crystal structure of complex [**12a**]OTf shows a strong Jahn–Teller distortion at the cobalt centre. The distance Co–O(H_2O) and Co–O(OTf) are 2.064(6) Å and 2.279(6) Å, respectively and the angle O–Co–O is 165°. Additionally, the two bipyridyl subunits are bent in a book-shaped fashion and out of the equatorial coordination plane by around 22°. The tetrapyridyl Co(II) moiety orients in an almost perpendicular fashion to the bis-benzene subunit.

Complex [**12a**]Br is photostable. Irradiation of a 20 μM solution in water with LED light at 453 nm (photon flux of 0.35 ± 0.02 μE s^{-1}) did not show any change in the UV spectrum after 8 h. After 24 h, minimal decomposition probably related to Co(II) decomplexation was observed (Fig. S20†). In addition, the UV/vis spectrum of complex [**12a**]Br did not change down to pH = 1.97 (Fig. S21†). Continuous additions of NaOH to a 20 μM solution lead though to irreversible changes in the UV/vis spectrum, indicating decomposition under strongly alkaline conditions (Fig. S22†).

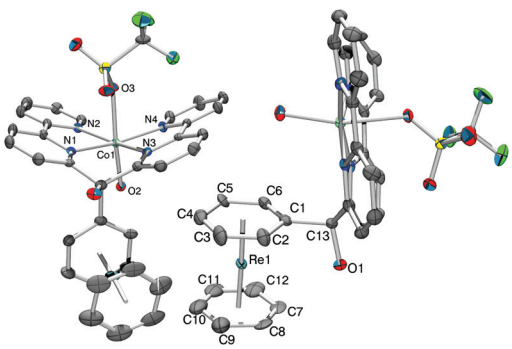

Fig. 3 ORTEP representation of the crystal structure of [**12a**]OTf along two different views. Hydrogen atoms and two OTf-anions have been omitted for clarity; thermal ellipsoids represent 40% probability. Selected bond lengths (Å): Re1–C1 2.252(8), Re1–C2 2.235(9), Re1–C3 2.218(10), Re1–C4 2.244(10), Re1–C5 2.259(10), Re1–C6 2.228(9), Re1–C7 2.228(10), Re1–C8 2.198(10), Re1–C9 2.206(13), Re1–C10 2.206(13), Re1–C11 2.238(11), Re1–C12 2.226(12), C1–C13 1.550(11), N1–C01 2.100(7), N–C01 2.108(7), N3–C01 2.103(7), N4–C01 2.109(7), Co1–O2 2.064(6), Co1–O3 2.279(6).

Photocatalysis

Since electronically decoupled, the pendent $[Re(\eta^6\text{-arene})_2]^+$ unit in **12a**$^+$ should not influence the activity of the catalyst. Accordingly, **12a**$^+$ was subjected to photocatalysis with $[Ru(bpy)_3]^{2+}$ as photosensitizer (PS) and ascorbate as the sacrificial electron donor (SED) (Scheme S1†). To regenerate dehydroascorbic acid (DHA), the oxidized form of ascorbate, tris(2-carboxyethyl)phosphine (TCEP) was added.[29–31,34] A comparison with the parent catalyst $[Co(Phbpy_2)Br_2]$ (**13**), *i.e.* **12a**$^+$ without $[Re(\eta^6\text{-arene})_2]^+$, was performed for assessing its innocence (Fig. 4 and Fig. S23†).

Accordingly, photocatalytic proton reduction experiments were performed with [**12a**]Br in water at pH 5, 0.1 M TCEP, 0.1 M NaAsc and 0.5 mM PS at five different concentrations of catalyst (1 μM, 5 μM, 10 μM, 20 μM, 100 μM). H_2 evolution was continuously monitored by in-line gas chromatography. Blank experiments in the absence of catalyst did not show significant amounts of H_2 formation in comparison to experiments with catalyst. Mercury poisoning experiments excluded the formation of nanoparticles as catalytically active species (Fig. S24†).

Fig. 4 shows a typical H_2 production profile as a function of time for 5 μM catalyst (for all concentrations, see Fig. S25†). The rate of H_2 evolution increases rapidly with time, reaching a maximum after around 2 h (for 5 μM of catalyst). Then, the H_2 formation rate decreases and catalysis ceases after 10 h. Depending on the WRC concentration, the periods of catalytic activities as well as the time needed for reaching the maximum turnover frequency (TOF) change. At higher initial concentrations of WRC, a delay until maximum TOF as well as longer catalysis time were observed, in line with previous studies by Joliat-Wick *et al.*[29]

Varying the concentrations of the WRC or the light intensity under otherwise identical condition are useful experiments to determine rate-limiting factors. As shown in Fig. 5a, the maximum TOF of H_2 formation stays about constant at around 520 h^{-1} for concentrations <10 μM, indicating either

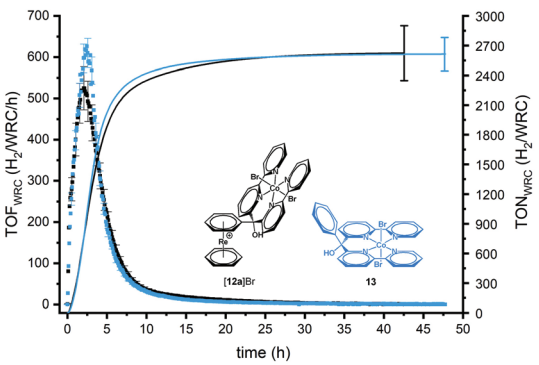

Fig. 4 Photocatalysis experiment with [**12a**]Br in black and the parent catalyst **13** in blue. TOF (dots) (H_2/Co/h) and TON (lines) (H_2/Co) formed as a function of time for 5 μM catalyst. Experimental conditions: 10 mL solution, 0.5 mM $[Ru(bpy)_3]Cl_2$, 0.1 M NaAsc, 0.1 M TCEP, pH 5.0, 453 nm LED irradiation.

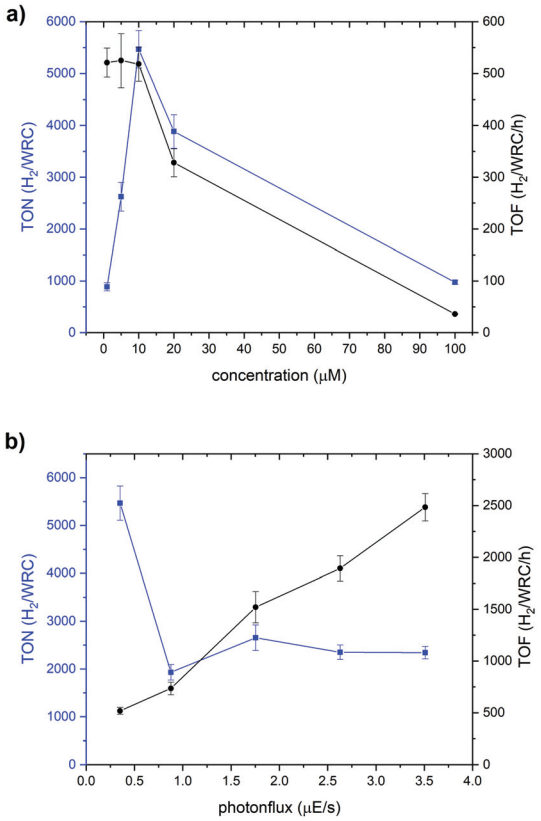

Fig. 5 TON and maximum TOF for H_2 evolution *vs.* (a) WRC concentration at a constant photon flux of 0.35 ± 0.02 μE s^{-1}. (b) photonflux with 10 μM of WRC. Experimental conditions: 10 mL of solution, 0.500 mM $[Ru(bpy)_3]Cl_2$, 0.1 M NaAscO, 0.1 M TCEP, pH 5.0, 453 nm LED irradiation. Black circles denote the maximum TOF of H_2 production and blue squares the turnover numbers.

electron transfer to or turnover of complex [**12a**]Br as rate limiting.

For concentrations above 10 μM, the TOFs decrease with increasing concentrations of WRC. At 20 μM and 100 μM, the maximum TOFs drop to 320 and 36 h^{-1} respectively. This effect is related to a limitation in the photocycle. At concentrations higher than 20 μM, the SED is almost completely consumed and for 100 μM in WRC, catalysis stops sharply after 70 h (Fig. S25b†) since no SED is available anymore. The limitation of the photocycle, *i.e.* the number of photons per time, can be shown by increasing the photon flux while keeping WRC concentrations constant. As obvious from Fig. 5b, TOFs increase linearly with increasing light intensity at 10 μM in WRC. A TOF of around 2500 h^{-1} is obtained upon irradiation of the sample with 3.5 μE s^{-1}, corroborating the limitations by the photocycle. Increased light intensities result in shorter but faster catalyses, overall with reduced TONs since higher photon fluxes favour the decomposition of the PS^-. All together, these observations support the view that the supply of electrons limits catalytic turnover frequency at concentrations below 10 μM and that the total photon flux limits it at higher concentrations. No negative interference with the

$[Re(\eta^6\text{-arene})_2]^+$ scaffold on the catalytic activity is observed as similar performances have been obtained for catalysts purely based on cobalt polypyridyl complexes.[29–31] Quantum yields were calculated from the maximum rate of H_2 formation and the number of absorbed photons. Two photons are required for one H_2 molecule. The quantum yields are between 1 and 10%, reaching the maximum at 20 μM in catalyst and 0.35 μE s^{-1} photonflux. Although catalyst **12a**$^+$ is relatively slow at low concentrations, the TONs and TOFs at higher concentrations are comparable with those of other systems with tetrapyridyl ligands.[30]

Conclusions

The sandwich complex $[Re(\eta^6\text{-arene})_2]^+$ represents a structural architecture to which additional functionalities such as ligands are conjugated in straight synthetic approaches. Additional reactive functions such as chlorides or aldehydes are introduced first on the arene rings, followed by ligand syntheses with these functions or, optionally, by direct coupling of intact ligands to the arenes. Thus, the respective opportunities provided by ferrocene are extended to $[Re(\eta^6\text{-arene})_2]^+$ scaffolds. The sandwich complex $[Re(\eta^6\text{-arene})_2]^+$ is cationic, which supports water solubility, and highly stable against redox reactions. Photocatalysis for H_2 formation corroborates the light stability of the entity and comparison with the parent catalyst, *i.e.* catalyst without the $[Re(\eta^6\text{-arene})_2]^+$ unit, confirms its purely structural role. We emphasize that the options offered by the $[Re(\eta^6\text{-}C_6H_6)_2]^+$ scaffold will go beyond the photocatalysis presented in this work. The high flexibility of the ligands to be conjugated can be equally exploited for other applications. Synergistic effects and communications between different modalities conjugated to the $[Re(\eta^6\text{-}C_6H_6)_2]^+$ scaffold is also anticipated.

Conflicts of interest

There are no conflicts to declare.

Acknowledgements

This study was financially supported by the University of Zurich, University Research Priority Project "LightChEC", and the Joint South Africa Switzerland Research Project IZLSZ2_170856 from the Swiss National Science Foundation.

Notes and references

1 E. O. Fischer and W. Hafner, *Z. Naturforsch., B: Anorg. Chem., Org. Chem., Biochem., Biophys., Biol.*, 1955, **10**, 665–668.
2 G. Pampaloni, *Coord. Chem. Rev.*, 2010, **254**, 402–419.
3 E. O. Fischer and A. Wirzmüller, *Chem. Ber.*, 1957, **90**, 1725–1730.
4 E. A. Trifonova, D. S. Perekalin, K. A. Lyssenko and A. R. Kudinov, *J. Organomet. Chem.*, 2013, **727**, 60–63.
5 G. Meola, H. Braband, P. Schmutz, M. Benz, B. Spingler and R. Alberto, *Inorg. Chem.*, 2016, **55**, 11131–11139.
6 M. Benz, H. Braband, P. Schmutz, J. Halter and R. Alberto, *Chem. Sci.*, 2015, **6**, 165–169.
7 D. Hernández-Valdés, G. Meola, H. Braband, B. Spingler and R. Alberto, *Organometallics*, 2018, **37**, 2910–2916.
8 A. Togni, *Angew. Chem., Int. Ed.*, 1996, **35**, 1475–1477.
9 F. Rebière, O. Riant, L. Ricard and H. B. Kagan, *Angew. Chem., Int. Ed.*, 1993, **32**, 568–570.
10 T. J. Colacot, *Chem. Rev.*, 2003, **103**, 3101–3118.
11 C. Ornelas, *New J. Chem.*, 2011, **35**, 1973–1985.
12 R. Djeda, A. Rapakousiou, L. Liang, N. Guidolin, J. Ruiz and D. Astruc, *Angew. Chem., Int. Ed.*, 2010, **49**, 8152–8156.
13 H. Yang, Z. Zhou, K. Huang, M. Yu, F. Li, T. Yi and C. Huang, *Org. Lett.*, 2007, **9**, 4729–4732.
14 D. Astruc, *Eur. J. Inorg. Chem.*, 2017, **2017**, 6–29.
15 D. R. Van Staveren and N. Metzler-Nolte, *Chem. Rev.*, 2004, **104**, 5931–5986.
16 G. Meola, H. Braband, S. Jordi, T. Fox, O. Blacque, B. Spingler and R. Alberto, *Dalton Trans.*, 2017, **46**, 14631–14637.
17 G. Meola, H. Braband, D. Hernández-Valdés, C. Gotzmann, T. Fox, B. Spingler and R. Alberto, *Inorg. Chem.*, 2017, **56**, 6297–6301.
18 S. M. Batterjee, M. Marzouk, M. Aazab and M. El-Hashash, *Appl. Organomet. Chem.*, 2003, **17**, 291–297.
19 M. Emilia, N. Silva, A. J. Pombeiro, J. J. F. da Silva, R. Herrmann, N. Deus, T. J. Castilho and M. F. C. Silva, *J. Organomet. Chem.*, 1991, **421**, 75–90.
20 M. E. N. Silva, A. J. Pombeiro, J. J. F. da Silva, R. Herrmann, N. Deus and R. E. Bozak, *J. Organomet. Chem.*, 1994, **480**, 81–90.
21 N. Queyriaux, R. T. Jane, J. Massin, V. Artero and M. Chavarot-Kerlidou, *Coord. Chem. Rev.*, 2015, **304–305**, 3–19.
22 C. Finn, S. Schnittger, L. J. Yellowlees and J. B. Love, *Chem. Commun.*, 2012, **48**, 1392–1399.
23 K. M. Waldie, A. L. Ostericher, M. H. Reineke, A. F. Sasayama and C. P. Kubiak, *ACS Catal.*, 2018, **8**, 1313–1324.
24 C. Costentin, G. Passard, M. Robert and J.-M. Savéant, *J. Am. Chem. Soc.*, 2014, **136**, 11821–11829.
25 K. E. Dalle, J. Warnan, J. J. Leung, B. Reuillard, I. S. Karmel and E. Reisner, *Chem. Rev.*, 2019, **119**, 2752–2875.
26 W. T. Eckenhoff, *Coord. Chem. Rev.*, 2018, **373**, 295–316.
27 Q. Nadeem, G. Meola, H. Braband, R. Bolliger, O. Blacque, D. Hernández-Valdés and R. Alberto, *Angew. Chem., Int. Ed.*, 2020, **59**, 1197–1200.
28 F. Kröhnke, W. Zecher, J. Curtze, D. Drechsler, K. Pfleghar, K. E. Schnalke and W. Weis, *Angew. Chem., Int. Ed.*, 1962, **1**, 626–632.
29 E. Joliat-Wick, N. Weder, D. Klose, C. Bachmann, B. Spingler, B. Probst and R. Alberto, *Inorg. Chem.*, 2018, **57**, 1651–1655.

30 S. Schnidrig, C. Bachmann, P. Müller, N. Weder, B. Spingler, E. Joliat-Wick, M. Mosberger, J. Windisch, R. Alberto and B. Probst, *ChemSusChem*, 2017, **10**, 4570–4580.
31 E. Joliat, S. Schnidrig, B. Probst, C. Bachmann, B. Spingler, K. K. Baldridge, F. von Rohr, A. Schilling and R. Alberto, *Dalton Trans.*, 2016, **45**, 1737–1745.
32 M. Guttentag, A. Rodenberg, C. Bachmann, A. Senn, P. Hamm and R. Alberto, *Dalton Trans.*, 2013, **42**, 334–337.
33 C. Bachmann, M. Guttentag, B. Spingler and R. Alberto, *Inorg. Chem.*, 2013, **52**, 6055–6061.
34 C. Bachmann, B. Probst, M. Guttentag and R. Alberto, *Chem. Commun.*, 2014, **50**, 6737–6739.